Calculated static and dynamic properties of β-Sn and Sn-O compounds

E. L. Peltzer y Blancá,* A. Svane, and N. E. Christensen†

Institute of Physics and Astronomy, Aarhus University, DK-8000 Aarhus C, Denmark

C. O. Rodríguez and O. M. Cappannini

Instituto de Física de Liquidos y Sistemas Biológicos, University of La Plata, 1900 La Plata, Argentina

M. S. Moreno

Department of Physics, University of La Plata, 1900 La Plata, Argentina

(Received 17 May 1993)

The static and dynamic properties of β-Sn, SnO, and SnO_2 are studied using the full-potential linear-muffin-tin-orbital method within the local-density approximation (LDA). Equilibrium lattice parameters and bulk moduli (including pressure variations) are in excellent agreement with experimental values. The cohesive energies are calculated too large, in accordance with the usual overbinding found in the LDA. Optical Γ-point phonon frequencies are obtained using the frozen phonon approach. For those phonon modes which have been measured, experimental identifications are confirmed, with the single exception of the B_{1g} mode of SnO, for which we find a frequency that is three times larger than the measured value. It is argued that the assignment of the observed mode is wrong.

I. INTRODUCTION

Two stoichiometric tin oxide compounds, SnO and SnO_2, are known to crystallize under ambient conditions in the tetragonal litharge and rutile structures, respectively.[1] Of these, SnO_2 is of considerable technological interest due to its applications in heat-reflecting filters, as transparent electrodes and in SnO_2/Si solar cells. Structural phase transitions to orthorhombic crystal structures as a function of pressure are observed for both compounds,[2,3] but the knowledge about these high-pressure phases and the phase transitions is still scarce. They are of significant importance in geophysical studies of mantle processes. Likewise, the oxidation process SnO→SnO_2 is still poorly understood. Intermediate phases of Sn_3O_4 and Sn_2O_3 have been suggested, but their crystal parameters are unknown.[4,5]

In the present work we study the electronic structure of β-Sn, SnO, and SnO_2 based on first-principles solid-state calculations with the aim of understanding the bonding properties of these compounds better. In particular, we focus our attention on the lattice parameters and their pressure dependence together with optical phonon frequencies. For our study the local approximation to the density functional theory[6] [i.e., the local-density approximation (LDA)] has been adopted. The effective one-particle equations are solved by means of the linear-muffin-tin-orbital (LMTO) method[7] in the full-potential version (FP-LMTO).[8,9] The FP-LMTO method was recently developed, and has proven to be fast and very precise. In contrast to the widely used LMTO-ASA (i.e., atomic spheres approximation), the FP-LMTO method does not make any shape approximations for the charge density and the potential. In the FP-LMTO method the crystal volume is divided into nonoverlapping muffin-tin spheres centered on each atom, and an interstitial region. The spheres are used for the definition of the basis set.

Inside the spheres the LMTO basis functions are represented by products of spherical harmonics and radial solutions to the scalar-relativistic Dirac equation. These functions are matched onto Hankel functions in the interstitial region. To achieve a basis set sufficiently complete for calculations of accurate total energies, Hankel functions with different characteristic decay constants are used. A full description and discussion of the FP-LMTO method is given in Refs. 8 and 9.

A basic assumption of the present work is that *differences* in total energy of the crystalline system in slightly different atomic arrangements may be calculated very accurately with the FP-LMTO and LDA schemes. To obtain optical phonon frequencies we employ the frozen phonon approximation,[10] which is based on the Born-Oppenheimer approximation, i.e., the total energy is computed as a function of the amplitude of the phonon mode considered with all other parameters of the calculation kept fixed. In the harmonic limit the phonon frequency is proportional to the square root of the distortion energy. The accuracy of the theoretical model adopted is checked against experimental knowledge about β-Sn, SnO, and SnO_2. This generally successful comparison lends confidence to the predictions of the theory concerning properties not experimentally investigated.

Several studies of tin and its oxides, SnO and SnO_2 have been reported. The different phases of tin have been investigated theoretically[11-13] as well as experimentally[14,15] and some optical Γ-point phonon frequencies have been measured[16,17] and calculated.[12,13] The static properties of SnO have been measured in Ref. 2 as a function of pressure and some measured phonon frequencies are reported by Ref. 4. Theoretical studies of this compound are to our knowledge restricted to cluster calculations of the density of states[18,19] and the Sn electric field gradient.[19] The SnO_2 compound has been more intensively studied than SnO. Experimentally, the static properties of

SnO_2 have been studied as a function of pressure,[20] while phonon frequencies are measured by,[4,21,22] the latter of which also considers the temperature and pressure dependencies. Theoretical studies of the electronic structure of SnO_2 have been performed by means of LMTO-ASA (atomic sphere approximation) calculations.[23,24] The semiempirical rigid ion model is considered in Refs. 21 and 25 to compute vibration frequencies, Grüneisen parameters and deformation potentials.

II. RESULTS

A. Static properties

β-Sn, SnO, and SnO_2 all belong to the tetragonal crystal systems, see Fig. 1. For β-Sn, the Bravais lattice is actually body-centered tetragonal (bct), with a c/a ratio of 0.543 and two tin atoms per bct unit cell at positions (0,0,0) and $(\frac{1}{2}a,0,\frac{1}{4}c)$. For SnO, the c/a ratio is 1.271 and the tetragonal unit cell contains two formula units with oxygen atoms placed at (0,0,0) and $(\frac{1}{2}a,\frac{1}{2}a,0)$, and tin atoms at $(0,\frac{1}{2}a,uc)$, and $(\frac{1}{2}a,0,-uc)$ with $u=0.238$.[26] The resulting litharge structure, also found for α-PbO, is highly layered with strong anisotropy, for instance in uniaxial compressibilities.[2] SnO_2 has $c/a=0.673$ and two formula units per tetragonal cell, with the tin atoms in bct positions (0,0,0) and $(\frac{1}{2}a,\frac{1}{2}a,\frac{1}{2}c)$ and the oxygen atoms in $\pm(ua,ua,0)$ and $(\frac{1}{2}a,\frac{1}{2}a,\frac{1}{2}c)\pm(ua,-ua,0)$, with $u=0.306$. These parameters lead to a nearly ideal octahedral coordination of the Sn atoms in SnO_2.

In Table I are shown the calculated values for these structural parameters together with experimental values. The theoretical values are obtained by doing self-consistent FP-LMTO calculations for a sequence of values of u, a, and c and finding the least-squares minimum of the total energy. For the calculation of SnO_2 all three parameters were varied freely, while we for SnO chose to fix u by requiring the nearest-neighbor Sn-O and O-O distances to be at a constant ratio. This corresponds to assuming that the product $u(c/a)$ is invariant to pressure. It is seen from Table I that all structural parameters are calculated within 1% of the experimental value, with the exception of the c/a ratio of SnO, which is calculated 4% lower than observed. The bulk moduli generally are calculated too low in compar-
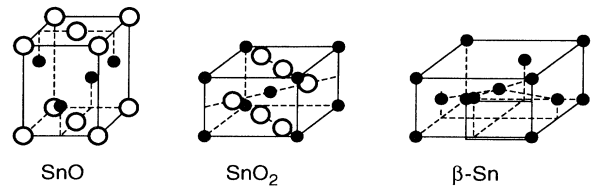
FIG. 1. Unit cells of tetragonal SnO and SnO_2 and β-Sn. Open circles are O atoms; full circles are Sn atoms.

ison with experimental values, by 8, 30, and 17% for β-Sn, SnO and SnO_2, respectively.

In Table II the calculated and measured volume derivatives of the lattice constants are given. It is observed that the β-Sn c/a ratio hardly changes with pressure (i.e., $d\ln c/d\ln V=d\ln a/d\ln V=\frac{1}{3}$), which is found both experimentally and theoretically. In contrast, for SnO the compressibility is very anisotropic. In the calculations, the compressibility along the c direction is five times larger than along the a direction. Experimentally, only contraction along the c direction is observed.[2,28,29] This reflects the fact that with pressure the SnO layers are brought closer together with hardly any alteration of the individual layers. SnO_2 is likewise found to be more compressible in the c direction in the present theoretical study, but this behavior is contradicted by experiments[20,30] on this compound, which find c/a increasing with pressure ($d\ln c/d\ln V < d\ln a/d\ln V$). The latter of these works even finds $d\ln c/d\ln V<0$,[30] which means that the c axis increases with increasing pressure. One should bear in mind, though, that greater uncertainties are involved in both measuring and calculating derivative properties.

In Table III cohesive energies of β-Sn, SnO, and SnO_2 are compared. Also listed are the decomposition enthalpies[32] of SnO and SnO_2, i.e., the energies required to accomplish the reactions

$$2SnO \rightarrow 2\beta\text{-Sn} + O_2$$

$$2SnO_2 \rightarrow 2SnO + O_2 .$$
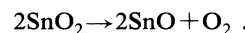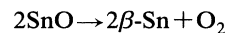
For these quantities the reference materials are the bulk solids and molecular oxygen gas, rather than the free atoms. Therefore the measured and calculated (in LDA) binding energy of the O_2 molecule is also quoted in Table

TABLE I. Static properties of β-Sn, SnO, and SnO_2.

| | u | | a (Å) | | c/a | | B (Mbar) | |
	Expt.	Theor.	Expt.	Theor.	Expt.	Theor.	Expt.	Theor.
β-Sn			5.8119[a]	5.865	0.543[a]	0.541	0.58[a]	0.54
SnO	0.2383[b]	0.2404	3.8029[b]	3.797	1.2722[b]	1.225	0.50[c]	0.35
							0.51[d]	
SnO_2	0.3064[e]	0.3061	4.737[e]	4.761	0.6726[e]	0.6687	2.18[e]	1.81

[a]Reference 27.
[b]Reference 26.
[c]References 2 and 28.
[d]Reference 29.
[e]Reference 20.

TABLE II. Volume derivatives of lattice parameters in β-Sn, SnO, and SnO$_2$.

| | $\dfrac{d \ln a}{d \ln V}$ | | $\dfrac{d \ln c}{d \ln V}$ | |
	Expt.	Theor.	Expt.	Theor.
β-Sn	0.32[a]	0.33	0.36[a]	0.33
SnO	0.17[b]	0.14	0.66[b]	0.73
	0.0[c]		1.00[c]	
SnO$_2$	0.42[d]	0.19	0.17[d]	0.64

[a]Reference 27.
[b]Reference 29.
[c]References 2 and 28.
[d]Reference 20.

III.

The well-established deficiency of the LDA approach of overestimating solid binding energies is also reflected in the data of the present calculations. The β-Sn cohesive energy is 14% too large according to theory, while the cohesive energies of SnO and SnO$_2$ are calculated $\sim$25% too large. It appears, that oxygen poses particular problems in the LDA, as is also reflected in the O$_2$ molecule data. The decomposition enthalpy of SnO$_2$ is well reproduced in the present approach, while the SnO decomposition enthalpy is calculated $\sim$1 eV too large. As a consequence, the disintegration energy for the process

$$2\text{SnO} \rightarrow \beta\text{Sn} + \text{SnO}_2$$

is calculated to be -0.50 eV (i.e., SnO is stable with respect to this decomposition), while the experimental value is $+0.04$ eV. Thus, the present calculation fails in predicting the instability of SnO.

In Figs. 2 and 3 the band structures of SnO and SnO$_2$ are shown, while Figs. 4 and 5 show the densities of states. For both compounds a gap is found between valence and conduction states. In SnO this gap is indirect and only 0.13 eV, while the minimum direct gap is 1.99 eV. In SnO$_2$ the minimum gap is 1.08 eV and direct at the Γ point. Experimentally, the gap of SnO has been measured by optical absorption to be 2.5–3 eV,[35] while

TABLE III. Experimental and theoretical cohesive energies and decomposition enthalpies of β-Sn, SnO, and SnO$_2$. Cohesive energies are in eV per Sn atom, or per SnO, SnO$_2$, or O$_2$ unit. Decomposition enthalpies are in eV per O$_2$ molecule. The theoretical cohesive energies include atomic spin-polarization energy (0.51 eV for Sn and 1.14 eV for O). Contributions from vibrations have not been taken into account.

| | E_{coh} | | E_{dec} | |
	Expt.	Theor.	Expt.	Theor.
β-Sn	3.14[a]	3.59		
SnO	8.73[b]	10.88	5.99[c]	6.84
SnO$_2$	14.36[b]	17.67	6.03[c]	5.84
O$_2$	5.22[d]	7.45[e]		

[a]Reference 31.
[b]Combination of data of Refs. 31, 32, and 33.
[c]Reference 32.
[d]Reference 33.
[e]Reference 34.
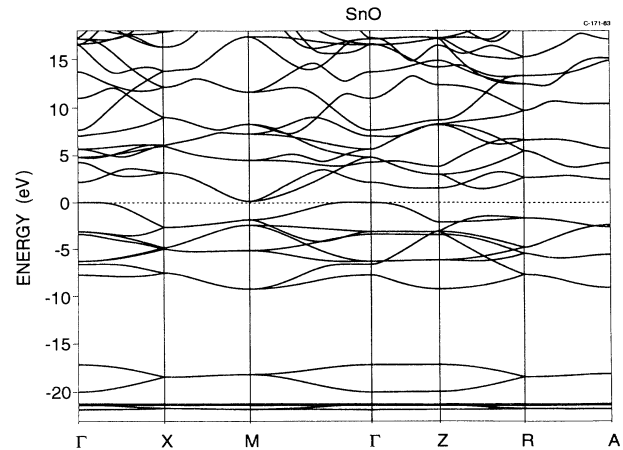
FIG. 2. Band structure of SnO. Units are eV relative to the valence band top. The zone edge points are $\Gamma(0,0,0)$, $X(1,0,0)$, $M(1,1,0)$, $Z(0,0,a/c)$, $R(1,0,a/c)$, and $A(1,1,a/c)$ in units of π/a.

the minimum gap of SnO$_2$ is found to be 3.6 eV.[36] Thus, the general tendency of underestimation of insulating gaps by the LDA energy eigenvalues[37,38] is also observed in the present calculations. The widths of the oxygen p bands are 8.9 and 8.4 eV for SnO and SnO$_2$, respectively. In a previous calculation of SnO$_2$,[23] the band width was found to be only 6.6 eV, an effect that is caused by the treatment of the Sn $4d$ semicore states as frozen-core states in that work. In the present work we have found it imperative to treat the Sn $4d$ states as part of the valence states. For this reason, the O p band width of SnO$_2$ of Ref. [24] is also in much better accord with the present calculation. The significant Sn d band width and Sn d–O s interaction is evident from Figs. 2 and 3. The calculated Sn d band widths are 1.0 eV and 2.2 eV for SnO and SnO$_2$, respectively, while the Os band widths are calculated to be 2.9 eV in SnO and 4.1 eV in SnO$_2$. The Sn $4d$ states are located at 20.3 eV and 19.1 eV below the
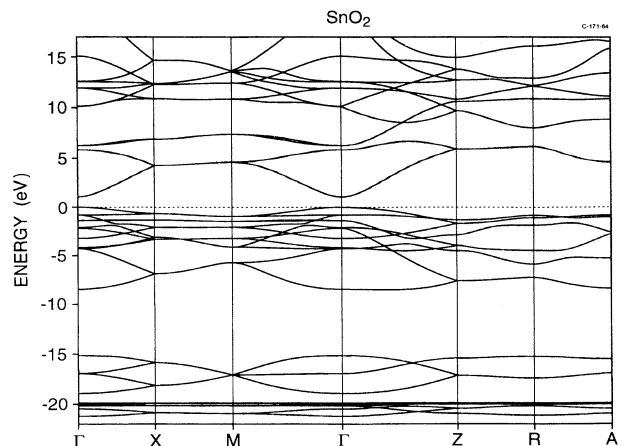
FIG. 3. Band structure of SnO$_2$. Units and definitions as in Fig. 2.
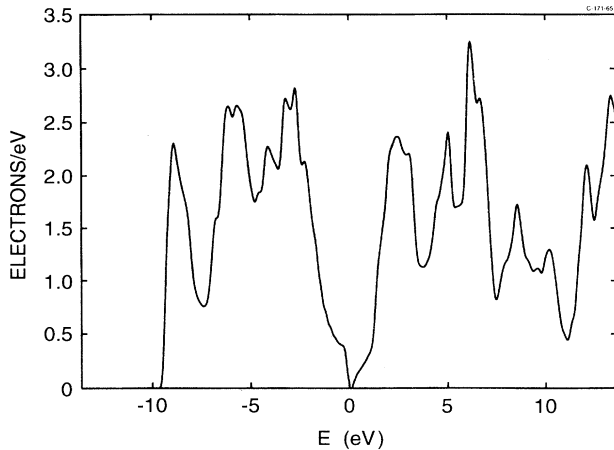
FIG. 4. Density of states for SnO. Energy is measured in eV relative to the valence-band maximum. Units for the density of states (DOS) is electrons per eV and unit cell. The deep Sn d and O s states are not shown.

O p valence band maximum in SnO and SnO_2, respectively. Synchrotron photoemission measurements on SnO_2 (Ref. 39) reveal an O p valence width of ~ 9 eV and a Sn $4d$ binding energy of ~ 23 eV, which is consistent with the present calculation, since an underestimation of core-state binding energies by a few eV by using the corresponding LDA eigenvalues has been found in similar cases.[37,38]

B. Phonon frequencies

The vibration frequencies of optical Γ-point phonons have been calculated in the frozen-phonon approach,[10] i.e., fixed phonon amplitudes are added to the atomic positions and the total energy of the electronic system is calculated self consistently. Subsequently, a harmonic fit is made to these energies as a function of phonon ampli-
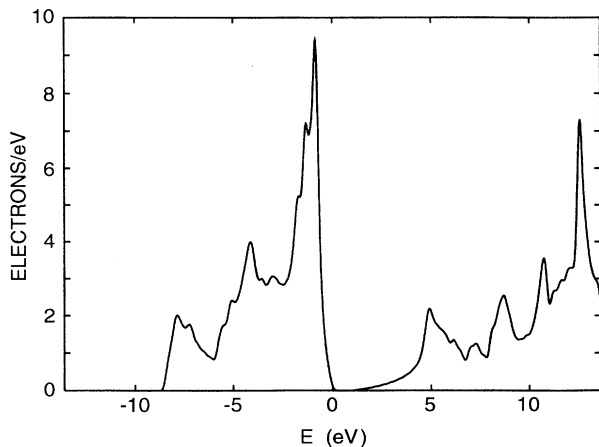
FIG. 5. Valence density of states for SnO_2. Energy is measured in eV relative to the valence band maximum. Units for the DOS is electrons per eV and unit cell. The deep Sn d and O s states are not shown.

TABLE IV. Optical Γ-point phonon frequencies of β-Sn in units of cm^{-1}.

	β-Sn		
Γ_5		Γ_3	
Expt.	Theor.	Expt.	Theor.
132.5[a]	130.0	46.50[a]	45.0
126.6[b]		42.44[b]	

[a]Reference 16.
[b]Reference 17.

tude. The results are reported in Tables IV–VI. The β-Sn frequencies in Table IV (cf. Fig. 6) are in extremely good agreement with experiment, and this also holds for the pressure derivatives hereof.[13]

The optical Γ-point phonon modes of SnO have been discussed in Ref. 4. Figure 7 shows the modes considered in the present work. The A_{1g}, A_{2u}, and B_{1g} modes are vibrations along the c axis, while the E_g and E_u modes involve movements in the xy plane. The A_{1g} mode is the symmetry preserving mode, where Sn atoms vibrate towards or away from the O plane, corresponding to variations in the u parameter. The B_{1g} mode consists of buckling vibrations of the O atoms out of their plane, while the A_{2u} mode describes rigid vibrations of the entire Sn sublattice with respect to the O sublattice along the c axis. Similarly, the E_u mode consists of rigid vibrations in the xy plane of the Sn sublattice with respect to the O sublattice, while the E_g mode involves vibrations within each sublattice and of one sublattice with respect to the other. Of these modes, the A_{1g}, B_{1g}, and E_g modes are Raman active, while A_{2u} and E_u are infrared active.

Table V quotes calculated frequencies of these modes together with experimental values of the A_{1g}, B_{1g}, and E_u modes,[4] which to our knowledge are the only experimental determinations of phonon frequencies in SnO. For comparison, the frequencies observed in the isostructural α-PbO are also given.[40] The calculated phonon frequencies are in excellent agreement with experiment for the A_{1g} and E_u modes (in particular when taking into account the larger experimental uncertainty on the frequency of the E_u mode, which is deferred from an infrared reflection experiment). On the other hand, the frequency

TABLE V. Optical Γ-point phonon frequencies of SnO in units of cm^{-1}. For comparison the measured frequencies of the isostructural α-PbO compound are also quoted.

	SnO		PbO
	Expt.[a]	Theor.	Expt.[b]
A_{1g}	211	211	150
B_{1g}	113	370	344
E_u	260	296	243
A_{2u}		396	116
E_g		143	83.4
E_g		494	327

[a]Reference 4.
[b]Reference 38.

E. L. PELTZER y BLANCÁ *et al.*

TABLE VI. Optical Γ-point phonon frequencies of SnO_2 in units of cm^{-1}.

	SnO_2 Expt.[a]	Theor.
A_{1g}	637	665
B_{2g}	781	760
E_g	476	518
B_{1g}	121	107
A_{2g}		353

[a]Reference 22.

of the B_{1g} mode is calculated to be more than three times larger than observed. Neither errors in the measurements nor computational errors are likely to explain this discrepancy, but we believe that the experimental assignment in Ref. 4 is incorrect: firstly, since B_{1g} is an O mode, while A_{1g} is a Sn mode, one would from the mass scaling alone $(\omega \sim 1/\sqrt{m}$) anticipate that the A_{1g} frequency is lower than the B_{1g} frequency.[40] This is indeed the order found in the present calculations. Secondly, since α-PbO is chemically similar to SnO, one would expect the interaction energies to be rather similar in the two compounds. Consequently, the energy variations as a function of frozen phonon amplitude should be very similar and oxygen modes have more or less the same frequency in PbO and SnO, while cation mode frequencies should scale with the cation mass to the power $-\frac{1}{2}$. Indeed, it follows from the data of Table V that for the experimental values for the A_{1g} mode, $\omega(SnO)/\omega(PbO) \sim 1.4$, while $\sqrt{m(Pb)/m(Sn)} \sim 1.32$. Similarly, for E_u, being predominantly an oxygen mode (the relevant mass for this mode is the reduced mass), $\omega(SnO) \sim \omega(PbO)$. But for the experimental values for the B_{1g} mode, the frequency in SnO is three times larger than the frequency in PbO. On the other hand, the calculated B_{1g} frequency is close to the frequency of this mode in PbO.

As an explanation for the line observed at $\omega = 113$ cm^{-1} we tentatively suggest that it actually is the low frequency E_g mode of SnO, which is seen. This mode has a calculated frequency of 143 cm^{-1} (cf. Table V). Another possibility is the occurrence of contamination with either β-Sn and/or SnO_2 in the SnO films studied in Ref. 4, since both the Γ_5 mode of the former (cf. Table IV) and the B_{1g} mode of the latter (cf. Table VI) have frequencies close to the observed value. Further experimental studies should be able to clarify this.
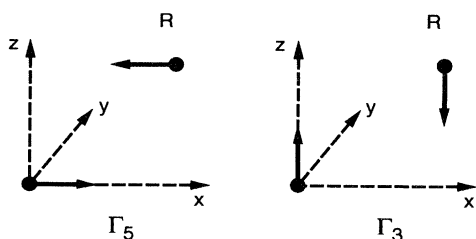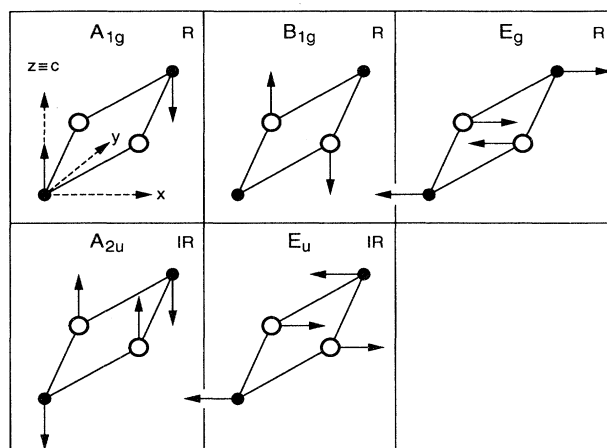
FIG. 7. Some optical Γ-point phonon modes of SnO.

Table V also gives calculated phonon frequencies for the A_{2u} and E_g modes, for which no experimental data have been published. The A_{2u} frequency is calculated somewhat higher than the E_u frequency, i.e., vibrations of the Sn sublattice with respect to the O sublattice is softer in the xy plane than in the z direction. For the E_g symmetry, a low-frequency mode at 143 cm^{-1} and a high-frequency mode at 494 cm^{-1} are calculated. In accordance with the mass argument above, the former mode is found to be dominated by Sn movement (displacements scale as $\delta_{Sn} = 24\delta_O$), while the latter mode is dominated by O movement. Comparing with α-PbO, the same splitting in a high and a low frequency of E_g symmetry is observed, but the experimental structure assigned to the A_{2u} mode is rather far from the calculated value in SnO. We have no explanation for this discrepancy, but recall that infrared reflection spectra (from which the A_{2u} frequency is deduced) are less well resolved than Raman spectra.

The optical Γ-point phonon modes of SnO_2 have been discussed in Refs. 21 and 41. In this work we have computed the frequencies of the four Raman active modes of SnO_2, the A_{1g}, B_{1g}, B_{2g}, and E_g modes, together with the A_{2g} mode; cf. Fig. 8. The results are given in Table VI

FIG. 6. Optical Γ-point phonon modes of β-Sn.
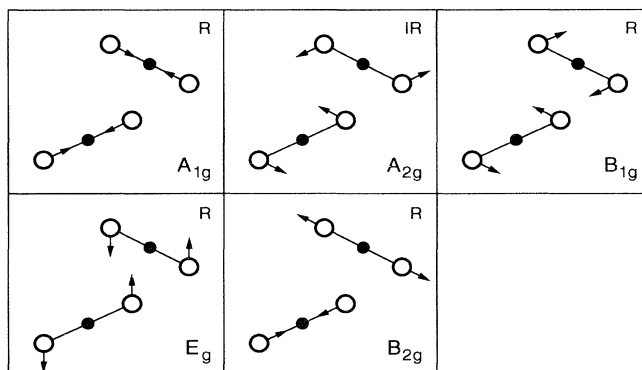
FIG. 8. Some optical Γ-point phonon modes of SnO_2.

together with the experimental value for the Raman active modes.[22] The A_{1g} is the symmetry preserving movement of the O atoms in the xy plane along the line through the nearest-neighbor Sn atom, which corresponds to oscillations in the u parameter. The B_{2g} mode consists of similar O oscillations, but in contrast to the A_{1g} mode, for the B_{2g} mode the vibrations of the two SnO_2 molecules ("rods") of the unit cell are in antiphase: if the O pair at $\pm(u,u,0)$ moves *towards* the Sn atom at the origin, the O pair at $\frac{1}{2}(a,a,c)\pm(u,-u,0)a$ moves *away* from the Sn atom at $\frac{1}{2}(a,a,c)$. The B_{1g} and A_{2g} modes correspond to rotational vibrations of the SnO_2 rods around the central Sn atom and in the xy plane, with the two rods of the unit cell rotating in phase (i.e., both clockwise or both counterclockwise) in the case of A_{2g} and in antiphase in the case of B_{1g}. Finally, the E_g mode corresponds to tilting of the rods out of the xy plane.

The calculated SnO_2 phonon frequencies of Table VI are in excellent agreement with the experimental Raman data. The A_{1g}, B_{2g}, and E_g frequencies are largest, since they involve stretching of the Sn-O bonds, while the B_{1g} and A_{2g} modes preserve the nearest-neighbor Sn-O distances to first order in the phonon amplitude. The fact that the frequencies of these two last modes are as different as found by the calculations [$\omega(A_{2g})=353$ cm^{-1}, $\omega(B_{1g})=107$ cm^{-1}], can be explained in terms of the O-O interactions. These modes only involve changing the distance between O atoms in adjacent z planes [next-nearest O neighbors, e.g., the O atom at $a(u,u,0)$ and the O atom at $a(\frac{1}{2}-u,\frac{1}{2}+u,\frac{1}{2}c/a)$]. The distance between these atoms is

$$R_{OO}=\tfrac{1}{2}a[1+(1-4u)^2+(c/a)^2]^{1/2} .$$

If we compute the derivative of this distance with respect to the phonon amplitude δ we find

$$\frac{dR_{OO}}{d\delta} \propto \begin{cases} 1 & \text{for } A_{2g} \\ 4u-1=0.23 & \text{for } B_{1g} . \end{cases}$$

Assuming, in a very simplified picture, that the interac-

tion energy depends quadratically on the next-nearest O-O distance only (since the nearest-neighbor O-Sn and O-O distances do not change to leading order in the phonon amplitude), we would expect the phonon frequencies to be in the same ratio: $\omega(B_{1g})/\omega(A_{2g})=4u-1$. Table VI shows that this is indeed the case, the calculated frequencies scaling as $\omega(B_{1g})/\omega(A_{2g})=0.30$.

III. CONCLUSION

In the present work the static and dynamic properties of β-Sn SnO, and SnO_2 have been calculated by use of the full-potential linear-muffin-tin-orbital method. A good agreement is found between theory and experiment for the structural parameters of these compounds, as well as for optical zone-center phonon frequencies. The only major discrepancy was found for the optical B_{1g} phonon mode of SnO, for which the theoretical frequency was found to be three times larger than the experimental value assigned to this mode. Several arguments have been presented to suggest that the experimental identification is in error. Comparing LDA eigenenergies to physical quasiparticle energies underestimates the fundamental energy gaps of SnO and SnO_2 as well as the binding energy of the localized Sn $4d$ states. Finally, for the cohesive energies $\sim 25\%$ overestimations were found for both SnO and SnO_2, which we attribute to errors inherent to the LDA. A consequence thereof is that SnO is erroneously calculated to be stable against decomposition into β-Sn and SnO_2

*Permanent address: IFLYSIB, University of La Plata, CC565, 1900 La Plata, Argentina.

†Also at Max-Planck-Institut FKF, D-7000 Stuttgart 80, Germany.

[1]R. W. G. Wykcoff, *Crystal Structures* (Wiley, New York, 1965), Vol. 1.

[2]D. M. Adams, A. G. Christy, J. Haines, and S. M. Clark, Phys. Rev. B **46**, 11358 (1992).

[3]K. Suito, N. Kawai, and Y. Masuda, Mater. Res. Bull. **10**, 677 (1975).

[4]J. Geurts, S. Rau, W. Richter, and F. J. Schmitte, Thin Solid Films **121**, 217 (1984).

[5]M. S. Moreno, R. C. Mercader, and A. G. Bibiloni, J. Phys. Condens. Matter **4**, 351 (1992).

[6]P. Hohenberg and W. Kohn, Phys. Rev. **136**, B864 (1964); W. Kohn and L. J. Sham, *ibid.* **140**, A1133 (1965).

[7]O. K. Andersen, Phys. Rev. B **12**, 3060 (1975).

[8]M. Methfessel, Phys. Rev. B **38**, 1537 (1988).

[9]M. Methfessel, C. O. Rodríguez, and O. K. Andersen, Phys. Rev. B **40**, 2009 (1989).

[10]H. Wendel and R. Martin, Phys. Rev. B **19**, 5251 (1979).

[11]C. O. Rodríguez, V. A. Kuz, E. L. Peltzer y Blancá, and O. M. Capannini, Phys. Rev. B **31**, 5327 (1985).

[12]B. H. Cheong and K. J. Chang, Phys. Rev. B **44**, 4103 (1991).

[13]N. E. Christensen and M. Methfessel, Phys. Rev. B **48**, 5797 (1993).

[14]S. N. Vaidya and G. C. Kennedy, J. Phys. Chem. Solids **31**, 2329 (1970).

[15]M. E. Cavaleri, T. G. Plymate, and J. H. Stout, J. Phys. Chem. Solids **49**, 945 (1988).

[16]J. M. Rowe, Phys. Rev. **163**, 547 (1967).

[17]H. Olijnyk, Phys. Rev. B **46**, 6589 (1992).

[18]P. M. A. Sherwood, Phys. Rev. B **41**, 10151 (1990).

[19]J. Terra and D. Guenzburger, Phys. Rev. B **44**, 8584 (1991).

[20]R. M. Hazen and L. W. Finger, J. Phys. Chem. Solids **42**, 143 (1981).

[21]R. S. Katiyar, P. Dawson, M. M. Hargreave, and G. R. Wilkinson, J. Phys. C **4**, 2421 (1971).

[22]P. S. Peercy and B. Morosin, Phys. Rev. B **7**, 2779 (1973).

[23]A. Svane and E. Antoncik, J. Phys. Chem. Solids **48**, 171 (1987).

[24]N. I. Mendvedeva, V. P. Zhukov, M. Ya. Khodes, and V. A. Goubanov, Phys. Status Solidi B **160**, 517 (1990).

[25]J. Pascual, J. Camassel, P. Merle, and H. Mathieu, J. Phys. (Paris) Colloq. **42**, Suppl. 12, C6-719 (1981).

[26]J. Pannetier and G. Denes, Acta Crystallogr. B **36**, 2763 (1980).

[27]J. A. Rayne and B. S. Chandrasekhar, Phys. Rev. **120**, 1658 (1960).

[28]The SnO compressibilities are taken from Fig. 5 of Ref. 2, which differs from the numbers in Table II of the same work. While the figure displays almost no variation in the a-parameter with pressure, the table quotes a substantial compressibility along a. If the numbers of the table are used one gets $B = 0.27$ Mbar and $d \ln a / d \ln V = 0.22$.

[29]L. F. Vereshchagin, S. S. Kabalkina, and L. M. Lityagina, Dokl. Akad. Nauk SSSR **163**, 326 (1966) [Sov. Phys. Dokl. **10**, 622 (1966)].

[30]H. G. Drickamer, R. W. Lynch, R. L. Clendenen, and E. A. Perez-Albuerne, Solid State Phys. **19**, 135 (1966).

[31]C. Kittel, *Introduction to Solid State Physics,* 5th ed. (Wiley, New York, 1976).

[32]O. Kubaschewski and B. E. Hopkins, *Oxidation of Metals and Alloys,* 2nd ed. (Butterworths, London, 1962).

[33]K. P. Huber and G. Herzberg, *Molecular Structure and Molecular Spectra, IV. Constants of Diatomic Molecules* (Van Nostrand Reinhold, New York, 1979).

[34]G. S. Painter and F. W. Averill, Phys. Rev. B **26**, 1781 (1982).

[35]As quoted by Ref. 4.

[36]V. T. Agekyan, Phys. Status Solidi A **43**, 11 (1975).

[37]R. O. Jones and O. Gunnarsson, Rev. Mod. Phys. **61**, 689 (1989).

[38]G. B. Bachelet and N. E. Christensen, Phys. Rev. B **31**, 879 (1985).

[39]P. L. Gobby and G. J. Lapeyre, in *Proceedings of the 13th International Conference on Semiconductors,* edited by F. Fumi (Rome, 1976), p. 150.

[40]D. M. Adams and D. C. Stevens, J. Chem. Soc. Dalton **1977**, 1096 (1977).

[41]C. Benoit and A. M. Vergnoux, J. Phys. (Paris) Colloq. Suppl. **27**, C2-35 (1966).